We would like to thank the reviewer for valuable comments and suggestions. We have addressed all raised issues in the revision accordingly. Please kindly find our following point-by-point responses. The reviewer's comments in black and our responses in blue. Any amendments in the revised manuscript are highlighted in red.

Response to Reviewer #1:

This manuscript investigated the aerosol composition and sources in Guangzhou, China, with a focus on ACSM measurements and subsequent PMF analysis. Routine analysis and plots were made. The conclusions are solid, but not exciting. However, latter part of the manuscript brought advance to the knowledge base by investigating the SOA sources and formation mechanisms from the perspective of RO2 chemistry. It is found that SOA has moderate correlation with RO2* in non-pollution days, but not in polluted episodes. Some conclusions are inferred by this analysis and I will discuss more later in the comment. This analysis distinguishes this manuscript from previous studies. I would like note that this type of novel analysis is missing from most of previous studies in China that are based on AMS+PMF analysis. Overall, I recommend publication with major revisions.

[A]: We would like to thank the reviewer for valuable comments and suggestions. Please find below our point-by-point responses.

Comments:

1. Even though the analysis on the relationship between SOA and RO$_2$ is novel, some discussions can be improved and I hope the authors will consider the following comments to make the manuscript hopefully more impactful. The major issue in this analysis is that SOA and RO$_2$ have dramatically different lifetime (days vs seconds). From this point of view, I find the moderate correlation between SOA and RO$_2$ in figure 10a and b intriguing, but hard to explain. My hypothesis for this correlation is that both SOA and RO2 are controlled by the amount of oxidants available. Another hypothesis is that they have similar diurnal variation (as shown in figure 5). It would be helpful to de-trend the SOA and RO$_2$ and then make the correlation analysis. For example, correlating SOA and RO$_2$ for data points at the same hour of day. In addition, the lifetime issue is especially important in polluted days when the air is more stagnant, SOA lingers for a long time, but RO$_2$ lifetime is short due to enhanced NOx concentration. This is likely the

main reason for the lack of correlation between SOA and RO_2 in polluted days (i.e., figure 10c and d, Page 17 Line 495). Overall, the different lifetimes of SOA and RO_2 should be kept in mind when interpreting any results.

[A]: We thank the reviewer for raising the important points on the correlations between SOA and RO_2*. We agree with the reviewer that lifetimes between SOA and RO_2^* are dramatically different. However, following the reviewer's suggestions, we further analyze the measurement data and find that the lifetime effects probably play a minor role in poor correlations between SOA and RO_2^* during pollution periods. Our results further confirm that gas-phase oxidation and gas-phase oxidation in combination with heterogenous reactions are respectively the main reasons for moderate correlations between SOA and RO_2^* during non-pollution periods and poor correlations during pollution periods.

(1) We believe that moderate correlations between SOA and RO_2^* in non-pollution period are due to gas-phase oxidation of VOCs that leads to formation of both RO_2^* and SOA (Details can be found in 147-159 in the revision). Thus, excluding heterogeneous reactions, intense gas phase oxidation (not only related to the amount of oxidants but VOCs) is expected to enhance the whole system of RO_2^*+SOA. Otherwise, both RO_2^* and SOA concentrations will decrease under weak gas phase oxidation. This is where the correlation between SOA and RO_2^* comes from.

According to the reviewer's suggestions, for the non-pollution period, we de-trended the correlations between the two species by plotting the dependence of SOA on RO_2^* concentration for the same short period (every 2 hours, to ensure enough points) of every day during non-pollution period in Fig. S13 (see it in supplementary or below). Like Figs. 10a and b in the manuscript, moderate correlations are seen from the de-trending plots. The results suggest the relationship between SOA and RO_2^*, especially the upward trend of SOA with increasing RO_2^*, is convincing. Thus, similar diurnal variations between SOA and RO_2^* in non-pollution period are the result of shared influence from gas phase oxidation of VOCs.
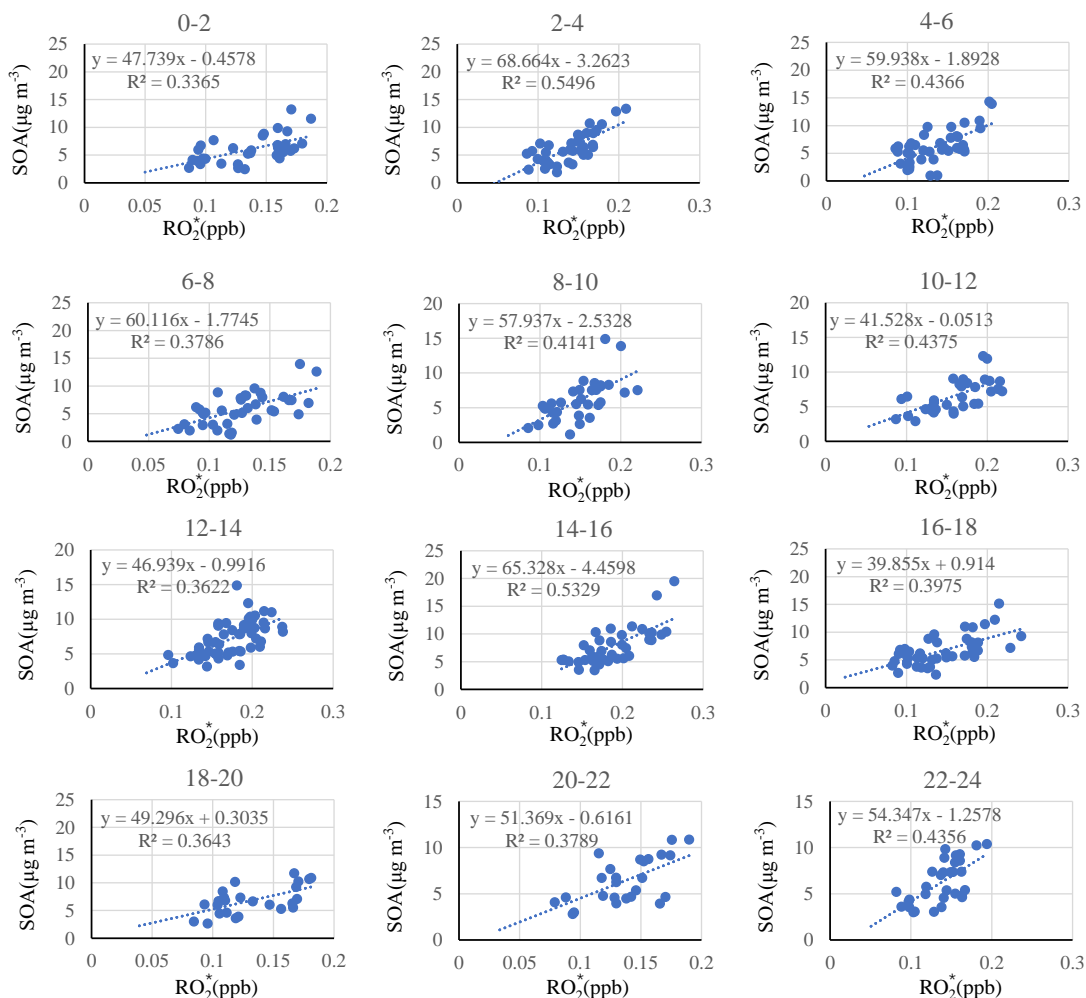
Figure S13. Dependence of SOA on RO_2^* concentration for the same short period of every day (i.e., every 2 hours) during non-pollution periods. Note that all the correlations are statistically significant (p-value < 0.01).

(2) During pollution periods, however, the correlations between SOA and RO_2^* become a little more complicated than those during non-pollution periods. We agree with the reviewer that lifetimes between SOA and RO_2^* are dramatically different (days vs seconds). However, here we show that the dramatic differences of lifetimes between the two species are not likely the main reasons which lead to poor correlations between them. As we mentioned in the paper, the odd oxygen ($O_x = O_3 + NO_2$) can be used as a robust photochemical indicator, which has a lifetime of about one day, a similar magnitude to that of SOA (Schaub et al., 2007; Lamsal et al., 2010; Valin et al., 2013). Here we present daytime relationship of O_x with SOA and RO_2^* during non-pollution and pollution EPs respectively (Fig. S14, see it in supplementary or below). Reasonably good correlations were found between RO_2^* and O_x during both non-pollution and pollution EPs. However, only reasonably good correlation between SOA and O_x was found during non-pollution periods, while no correlation at all was found during pollution EPs, neither

was found for the correlation between SOA and RO2* during pollution EPs (Fig. 10c in the revision). If the dramatic difference of lifetime was to play an important role in the correlation as the reviewer hypothesizes, the reasonably good correlation between RO2* and O_x in non-pollution period shouldn't exist during pollution EPs, just like what happen to RO2* and SOA. Besides, when we discuss the relationship between SOA and O_x (similar life time), the same pattern as that for SOA and RO2* (Fig. S15 c and d) is revealed. Hence, we believe that the lifetime effects probably play an insignificant role in the poor correlation between SOA and RO2* during pollution EPs. We think that no correlations between SOA and RO2*/Ox during pollution EPs implied dramatical changing of SOA formation mechanisms.

As the reviewer pointed out, the enhanced NO_x during polluted days would influence the lifetime of RO2*. As NO_x concentration increases, more RO2* was consumed. Then the correlation between RO_2^* and O_x (also SOA) may become worse with significantly enhanced NO_x levels. However, this influence is probably not significant in this study because a good correlation was still found between RO_2^* and O_x during pollution EPs (Fig. S15b).
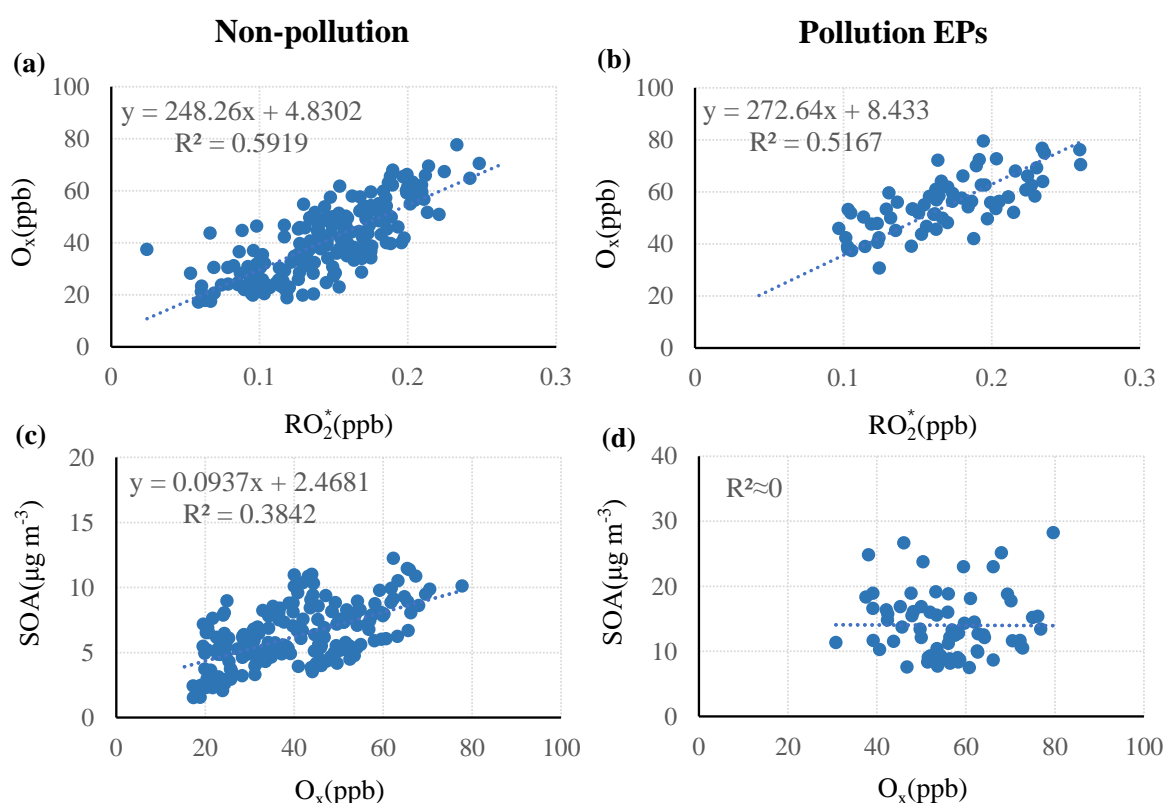
Figure S14. Daytime dependence of O_x on RO2* (a, b) and dependence of SOA on O_x (c, d) for pollution EPs and non-pollution period.

（3）We further confirm the distinctly different mechanisms for SOA formation between non-pollution and pollution EPs by plotting estimated H/C ratio as a function of O/C ratio in the Van Krevelen

diagram. The O/C and H/C ratios were estimated from f_{43} and f_{44}, which were proposed by Aiken et al. (2008) and Ng et al. (2011) respectively. Similar diagrams based on ACSM unit mass resolution data were reported in previous studies (Brito et al., 2014; Reece et al., 2017; Saha et al., 2018). The area enclosed by the two red boundary lines was defined for ambient OOA components in Ng et al. (2011). Our data points were slightly outside of this area and were further shifted to the upper right corner of the plot. Similar differences from other ambient or laboratory measurements were also reported in previous studies (Budisulistiorini et al., 2018; Saha et al., 2018), which were attributed to different precursors emitted or aging processes. As is shown in Fig. 11a (see it in revision or below), the H/C ratio is linearly correlated with the O/C ratio and is confined into a narrow belt during non-pollution periods, indicating the precursors, mechanism, and chemical components of SOA are likely similar (Ng et al. 2010, 2011). Although the H/C ratio follows similar trends with O/C ratio during pollution periods, the shape is much broader with respect to the H/C ratio especially in the middle portion of the O/C ratio, strongly indicating that more diverse components in SOA are present surrounding the measurement site in Guangzhou. A wider range of H/C ratio during pollution EPs imply more diverse precursor sources and (or) different mechanisms which lead to formation of SOA components with highly variable H/C ratios (Ng et al. 2010, 2011). Although we cannot totally rule out the possibility of dramatic changes in the emission sources, it is unlikely for those changes to occur within a month of the measurement period. Besides, it is unreasonable that these changes only coincidently happened in pollution EPs. Hence it is more likely that the formation mechanisms during non-pollution and pollution periods are distinctly different. Here we propose two most possible different mechanisms of SOA formation during pollution EPs: (1) gas-phase oxidation under enhanced NO_x concentration which leads to dramatically different SOA components from these under lower NO_x concentration (Ziemann et al., 2012); (2) other mechanisms such as additional heterogeneous/multiphase reactions from dramatic increases of PM mass loading and hence more available particle surfaces or volumes for reactions. We replot estimated H/C ratio vs estimated O/C ratio in the Van Krevelen diagram with an overlapped NO_x concentration range during the two periods to remove the enhanced NO_x effects (Fig. 11b). Similar patterns were obtained, highlighting the high possibility of significant heterogeneous/multiphase reactions in pollution EPs. A new Figure 11 and relevant content were added in the revised manuscript (lines 496-523, page 17).
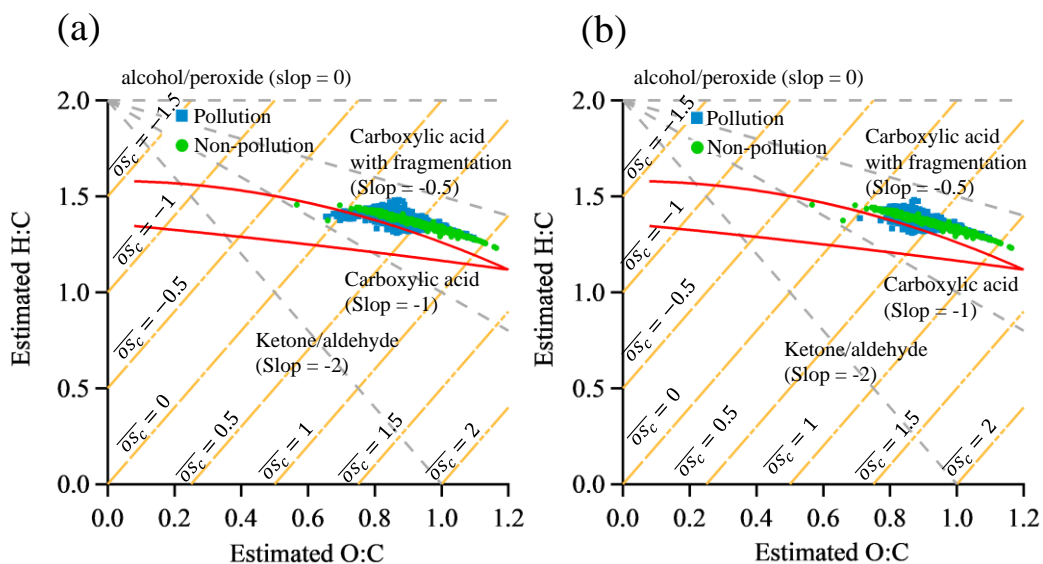
Figure 11. Plot of estimated H/C ratio as a funciton of estimated O/C ratio in the Van Krevelen diagram: (a) Non-pollution vs. pollution EPs; (b) Non-pollution vs. pollution EPs with an overlaped NO_x concentration range during the two periods. The area enclosed by the two red boundary lines was defined for ambient OOA components in Ng et al. (2011).

"We further investigate the distinctly different mechanisms for SOA formation between non-pollution and pollution EPs by plotting estimated H/C ratio as a function of O/C ratio in the Van Krevelen diagram (Fig.11). The O/C and H/C ratios were estimated from f_{43} and f_{44}, which were proposed by Aiken et al. (2008) and Ng et al. (2011) respectively. Similar diagrams based on ACSM unit mass resolution data were reported in previous studies (Brito et al., 2014; Reece et al., 2017; Saha et al., 2018). The area enclosed by the two red boundary lines was defined for ambient OOA components in Ng et al. (2011). Our data points were slightly outside of this area and were further shifted to the upper right corner of the plot. Similar differences from other ambient or laboratory measurements were also reported in previous studies (Budisulistiorini et al., 2018; Saha et al., 2018), which were attributed to different precursors emitted or aging processes. As shown in Fig. 11 a, the H/C ratio is linearly correlated with the O/C ratio and is confined into a narrow belt during non-pollution periods, indicating the precursors, mechanism, and chemical components of SOA are likely similar (Ng et al. 2010, 2011). Although the H/C ratio follows similar trends with O/C ratio during pollution periods, the shape is much broader with respect to the H/C ratio especially in the middle portion of the O/C ratio, strongly indicating that more diverse components in SOA are present surrounding the measurement site in Guangzhou. A wider range of H/C ratio during pollution EPs imply more diverse precursor sources and (or) different mechanisms which lead to

formation of SOA components with highly variable H/C ratios (Ng et al. 2010, 2011). Although we cannot totally rule out the possibility of dramatic changes in the emission sources, it is unlikely for those changes to occur within a month of the measurement period. Hence it is more likely that the formation mechanisms during non-pollution and pollution periods are distinctly different. Here we propose two most possible different mechanisms of SOA formation during pollution EPs: (1) gas-phase oxidation under enhanced NOx concentration which leads to dramatically different SOA components from these under lower NOx concentration (Ziemann et al., 2012); (2) other mechanisms such as additional heterogeneous/multiphase reactions from dramatic increases of PM mass loading and hence more available particle surfaces or volumes for reactions. We replot estimated H/C ratio vs estimated O/C ratio in the Van Krevelen diagram with an overlapped NOx concentration range during the two periods to remove the enhanced NOx effects (Fig. 11b). Similar patterns were obtained, highlighting the possibility of significant heterogeneous/multiphase reactions in the pollution EPs."

2. Correlation between RO_2 and O_3. Assume RO_2 is at steady-state, then we can approximate $d[RO2]/dt=k[O3][VOC]-k[RO2][NO]=0$ $[RO2]≈([O_3][VOC])/([NO])$ If the [VOC]/[NO] ratio doesn't change much, a correlation between RO_2 and O_3 may be expected. The equation here is over-simplified, but my point is that many discussions may start from or be explained by this type of simple mathematical derivation.

[A]: We thank the reviewer for valuable suggestions. According to recent measurements in Guangzhou, about 67%, 17% and 16% of VOCs are alkanes, alkenes and aromatic hydrocarbons respectively (Zou et al., 2015). Hence during daytime, it is likely that the predominant sources of RO_2* are from OH-initiated hydrocarbon oxidation, complicated by a probably minor contribution from ozone- alkene/aromatic hydrocarbon oxidation. In fact, based on previous VOCs (Zou et al., 2015) and OH (Rohrer et al., 2014) measurement data in Guangzhou, along with O_3 concentration in this study and rate constants reported in Atkinson et al. (2003), the OH contribution to RO_2* is estimated 100 times larger than O_3 contribution. During nighttime, however, since it is likely that the predominant sources of RO_2* are from NO_3-initiated hydrocarbon oxidation, along with a minor contribution from ozone-alkene/aromatic hydrocarbon oxidation (Volkamer et al., 2010; Stone et al., 2014). In either case, the relationship between RO_2* and ozone is not straightforward. Hence it is unlikely to connect them with a simple and explicit mathematical form.

In fact, in this paper, we employ O_x ($O_x = O_3 + NO_2$) instead of ozone itself as a proxy when discussing the effects of photochemistry on SOA formation (Herndon et al., 2008). Here NO_2 is used to compensate O_3 consumption. Here we plot O_x concentration as a function of RO_2^* concentration for different scenarios (non-pollution daytime, non-pollution nighttime, pollution daytime and pollution night time) (Fig. S4 a-d, see it in supplementary or below). The results show that good correlations between O_x and RO_2^* were only seen during daytime when photochemistry occurs while poor or no correlations at all were observed during nighttime when photochemistry is shut off. Interestingly, when we plot ozone concentration as a function of RO_2^* concentration for the four scenarios, good correlations between ozone and RO_2^* were all seen during regardless of daytime or nighttime (Fig. S4 e-h). As mentioned above, good correlation between RO_2^* and O_3 should come from shared photochemistry during daytime. In contrast, RO_2^* is mainly contributed by NO_3/O_3-initiated VOCs oxidation during nighttime. Previous studies have proved that nocturnal NO_3 radicals mainly comes from NO_2 oxidation by O_3, i.e., $NO_2 + O_3 = NO_3 + O_2$ (Volkamer et al., 2010; Stone et al., 2014). Thus, RO_2^* is always related to O_3 concentration at night, likely explaining their good nocturnal correlations.
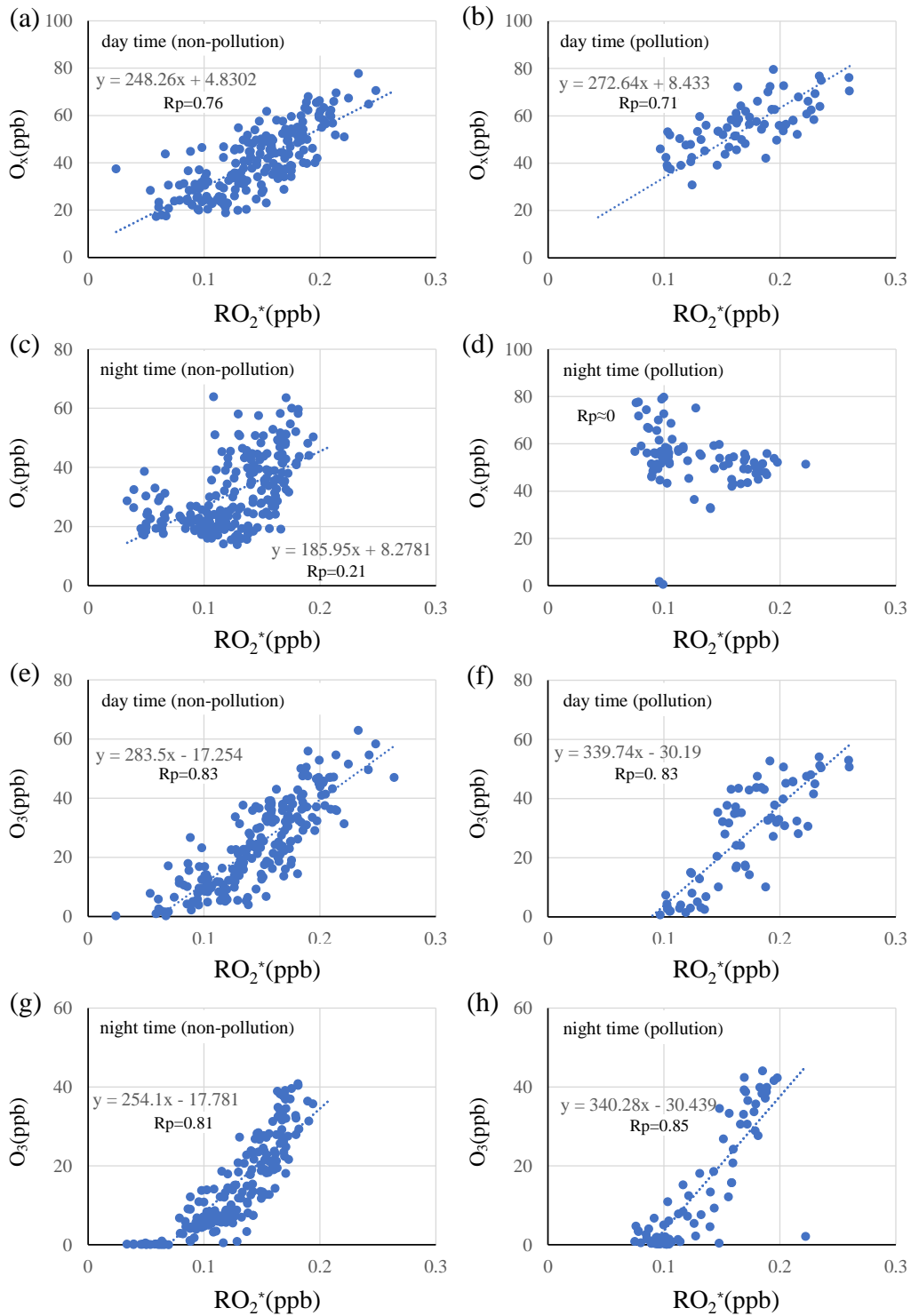
Figure S4. Dependence of O_x and O_3 on RO_2^* for different scenarios (non-pollution daytime period, pollution daytime EPs, non-pollution nighttime period, and pollution nighttime EPs). All the regressions are orthogonally linear.

3. In figure S4, the correlation between RO_2 and O_3 for the whole campaign is shown. I suggest the authors also categorize all data points into sub-groups (non-pollution vs polluted, day vs night, as figure 10) and show correlation relationship. The reason I suggest this is that based on figure 10c, polluted days only

account for a small fraction of all data points. Thus, the relationship between RO2 and O3 for polluted days are not clearly shown in the assembly of all data points.

[A]: According to the reviewer's suggestions, we have adjusted Figure S4 and showed the correlation between RO_2 and O_3 with subgroups. Please refer to answer #2.

4. Figure 11 and Page 17 Line 505. By eyeballing, the correlation between RO2 and SOA at each sub-group is very week. The p-value for linear regression must be included.

[A]: We included the p-values into Figure 11 in the original version (now Figure 12 in the revision).We also added a sentence to the caption of the figure, "all correlations of the concentration segments were statistically significant (p-value < 0.01, see detailed statistical information in Table S3)." Additionally, a table (Table S3) with detailed statistic information was added into the supplementary.

We agree with the reviewer that the correlations between SOA and RO_2* during pollution periods are not as strong as those during non-pollution periods probably due to fewer points. Nevertheless, we show that a more viable dependence trend of SOA on RO_2* in pollution EPs can be seen by dividing samples into 6 sub-groups based on different PM_1 mass intervals (Figure 12).

Table S3. P-value, T-value, number of points (n), and Pearson Correlations between SOA and RO_2* for different $NR\text{-}PM_1$ concentration intervals.

$NR\text{-}PM_1$ ($\mu g\ m^{-3}$)	r	n	T	p
< 30	0.31	47	5.07	<0.001
30-40	0.50	60	4.40	<0.001
40-50	0.53	35	3.56	0.0012
50-60	0.49	41	3.51	0.0011
60-70	0.62	40	4.93	<0.001
>70	0.59	30	3.85	<0.001
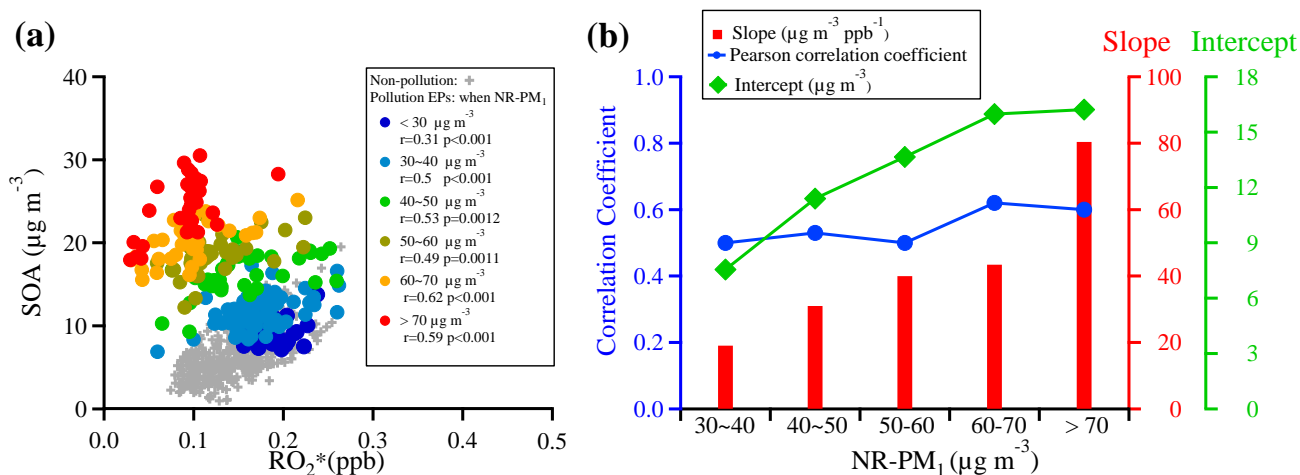
Figure 12. (a) Scatter plots of SOA and RO_2^* during pollution EPs at different $NR\text{-}PM_1$ mass concentration segments, and (b) Correlation coefficients, slopes, and intercepts of linear regressions between SOA and RO_2^* for $NR\text{-}PM_1$ mass concentration segments ranging from 30-40 to > 70 $\mu g\ m^{-3}$. The regressions are orthogonally linear, and all correlations of the concentration segments were statistically significant (p-value < 0.01, see detailed statistical information in Table S3).

5. Page 2 Line 62 and Page 17 Line 518. It is not clear why the intercept represents the extent of other SOA formation mechanisms. I think the related conclusions are overblown.

[A]: We thank the reviewer for pointing this out. As we show in answer #1 that that gas-phase oxidation and gas-phase oxidation in combination with heterogenous reactions are respectively the main reasons for moderate correlations between SOA and RO_2^* during non-pollution periods and poor correlations during pollution periods. As also mentioned in the above answer, although the correlations between SOA and RO_2^* during pollution periods are not as strong as those during non-pollution periods, the extrapolation of these regressions, that is, the intercepts might imply mechanisms of SOA formation as more SOA is formed with increasing PM concentrations. In addition, the intercept from the regressions between SOA and RO_2^* during non-pollution periods is essentially close to zero, leading us to believe that the intercepts likely correspond to the amount of SOA formed from other mechanisms (i.e., heterogenous reactions) other than gas-phase oxidation.

6. Page 17 Line 513: RO_2 concentration can not represent the amount of gas phase oxidation products

[A]: We agree with the reviewer and have removed the relevant sentence.

~~"We assume that RO2* can roughly represent the amount of gas phase oxidation products of VOCs which seems to be reasonable."~~

7. Figure 8. Please include all data points in this plot, in addition to the binned-average.

11

[A]: We thank the reviewer for the suggestion. We have modified Figure 8 in revision by including all data points and separating it into several panels. We have hence changed the caption of Figure 8 as shown below.
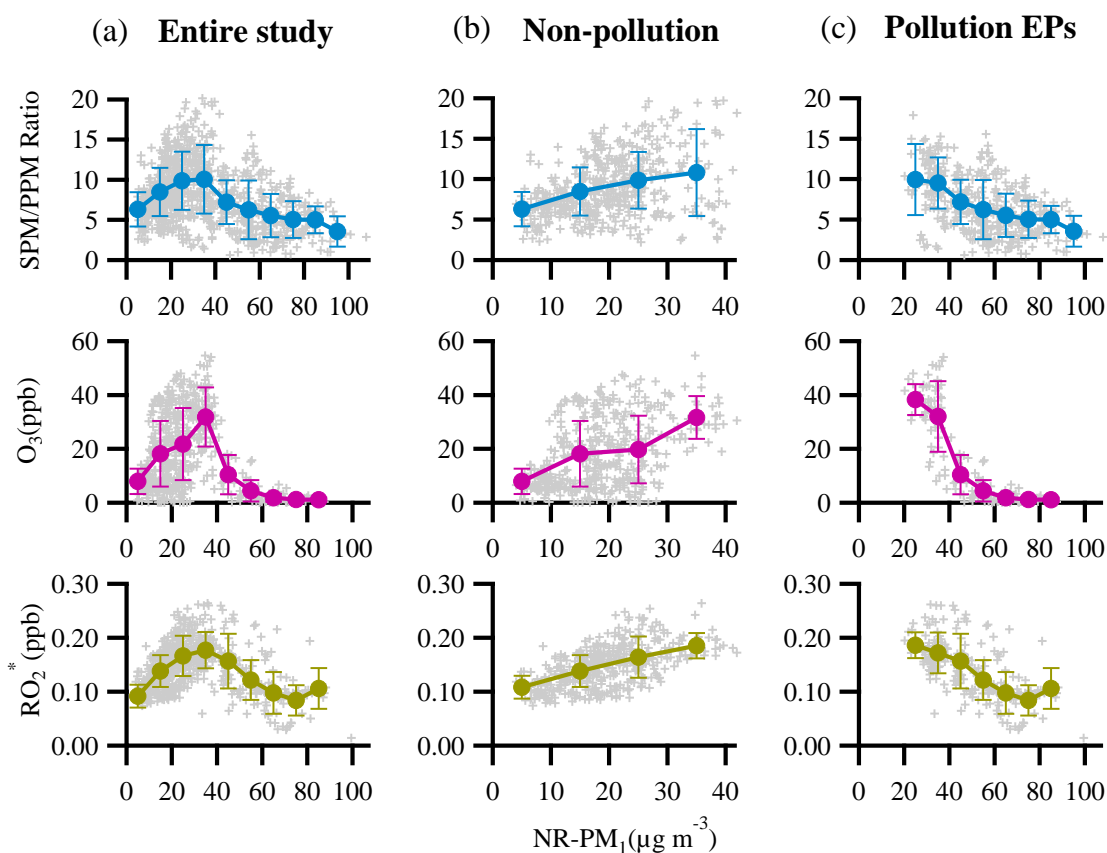
Figure 8. Dependences of SPM/PPM ratio, concentrations of the atmospheric oxidants (O_3 and RO_2^*) on NR-PM_1 mass loading for (a) entire study, (b) non-pollution period and (c) pollution EPs. The binned data are also presented as solid circles with an interval of 10 μg m^{-3} NR-PM_1. The error bars are standard deviations.

8. Figure 10 and 11 and S4. Please use orthogonal linear regression, which considers the measurement uncertainty in both x- and y-axis.

[A]: Per the reviewer's suggestions, we have replaced Figure 10, Figure 11 (now Figure 12 in the revision), and Figure S4 using orthogonal linear regressions (Minitab 2019, www.minitab.com). The renewed figures don't change our original conclusions. We also mentioned this in captions of these figures.

Minor Comments

1. Page 4 Line 102: I believe the authors mean "inevitable", instead of "evitable".

[A]: Corrected (line 103, page 4).

2. Page 6 Line 175: Even though the measurement details of RO2* have been described in previous studies, it is still beneficial to briefly mention how the measurements were done.

[A]: Agree, we have added several sentences to describe the measurement details of RO_2* in the revision (lines 194-200, page 7).

"The concentrations of the total peroxy radicals (RO_2* = $\Sigma RO_2^{\cdot}$+HO_2) were measured with a dual-channel PERCA (Peroxy Radical Chemical Amplification) instrument (Yang et al., 2018; Yang et al., 2019). In this instrument, ambient mixing ratios of RO_2* radicals were converted to a larger amount of NO_2 by reacting with NO and CO. The amplified NO_2 concentrations were then measured with a portable broadband cavity enhanced spectrometer (BBCES) with a precision of 40 pptv (1σ, with 21 s data acquisition time) (Fang, et al., 2017). The total uncertainty of the PERCA instrument was about 10% with a precision of about 0.4 pptv (1σ, 21 s)."

3. Page 9 Line 254: The selection of a-value should be justified.

[A]: We thank the reviewer for pointing this out. We have now added several sentences in supplementary in the method section, "The results showed that an unreasonably high proportion of m/z 44 were presented in COA profiles for solutions with a-values of 0.5 and 0.7. We hence adopt 4 factors and an a-value of 0.3 as the optimal solution. The results from ME-2 are shown in Figures S5-S11".

In addition, we have also added one sentence in the revision (lines 278-279, page 9), "Detailed selection of a-value can be found in supplementary (method section)."

4. Page 9 Line 274: Even in non-pollution period, rush hour peaks in HOA are expected. Thus, the lack of diurnal variation in HOA in this study is alarming. It may be due to the low resolution of ACSM.

[A]: We agree with the reviewer that the resolution of ACSM is low compared to regular AMS. The HOA concentration during non-pollution periods after ME-2 factorization is low (< 1 μg m^{-3}), close to an estimated detection limit of 0.7 μg m^{-3} for OA, leading to lack of diurnal variations in HOA. However, it is unlikely to affect other organic factors since the concentrations of other organic components are much higher than the estimated detection limit for OA.

For clarification, we have added several sentences in the revision (lines 299-302, page 10), "In comparison, the HOA concentration showed almost no variations during non-pollution period (even

during rush hours), which likely arose from its extremely low value (< 1 µg m^{-3} which was close to an estimated detection limit of 0.7 µg m^{-3} for OA with the ToF-ACSM)."

5. Page 10 Line 307: Replace "high volatility" with "semi-volatile".

[A]: We have corrected it (line 333, page 11).

6. Page 16 Line 490: the trend between f44 and SOA concentration is not clear in figure 10. Regarding the claimed conclusion that f44 of SOA decreases with increase of SOA concentration, I suggest the authors to check if there is any "contamination" in PMF analysis. In other words, in polluted days, is some POA apportioned into SOA by PMF analysis? This can be done by either run PMF on non-pollution and polluted days separately and see if the fraction of SOA changed, or check the residual of POA characteristic ions during polluted days. The former approach is more reliable.

[A]: According to the reviewer's suggestions, we plotted the dependence of SOA concentration on f44 for different scenarios (non-pollution daytime, non-pollution nighttime, pollution daytime and pollution night time) as is shown in Fig. S16 (see it in supplementary or below). The trends between SOA and f44 are clear: SOA concentrations increase with increasing f44 during non-pollution periods while opposite trends are observed during pollution periods. In addition, we ran Me-2 separately for non-pollution periods and pollution EPs (Fig. S17, see it in supplementary or below). The results from those additional runs show similar fractions and concentrations of SOA, confirming reliability of our original results.

14
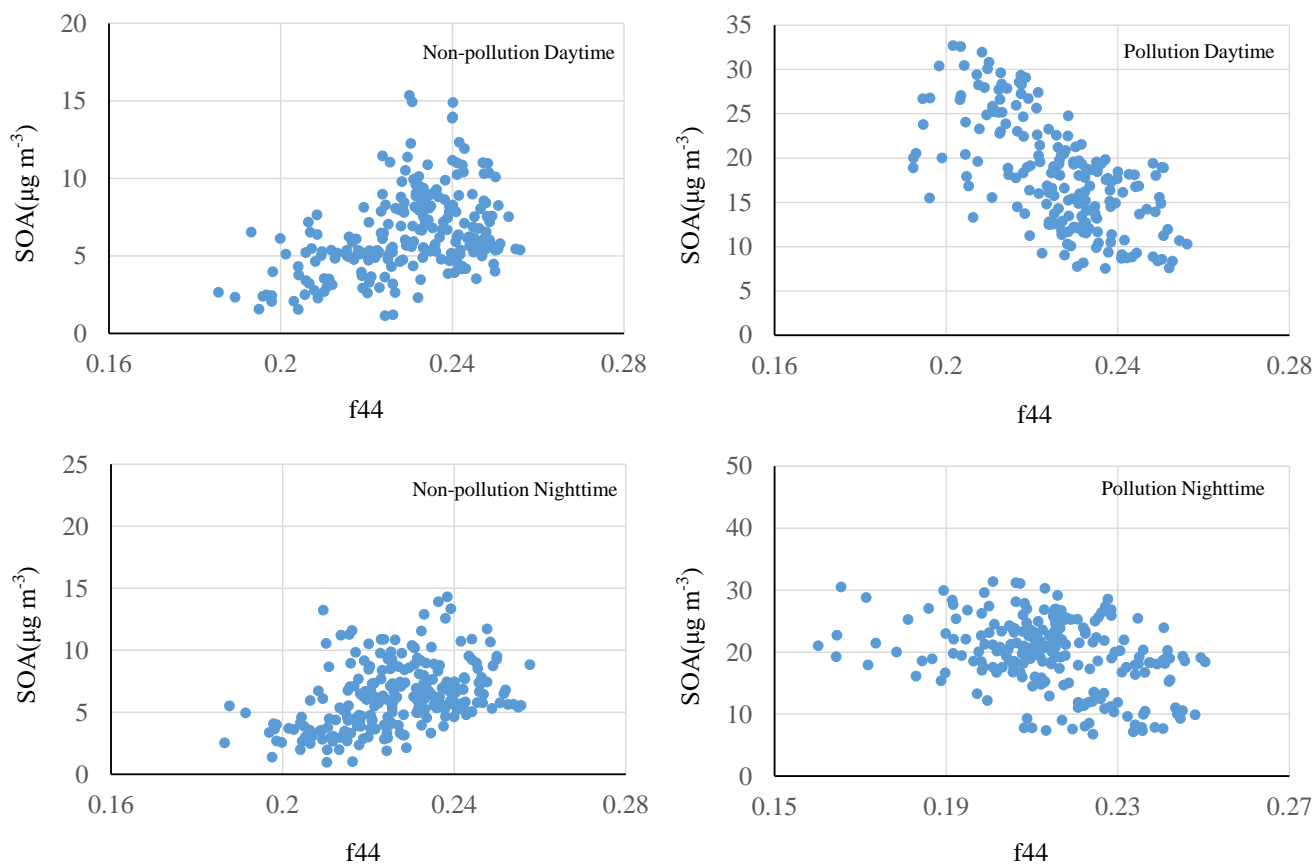
Figure S16. Scatter plots between SOA and f44 for different scenarios (non-pollution daytime, non-pollution nighttime, pollution daytime and pollution night time).
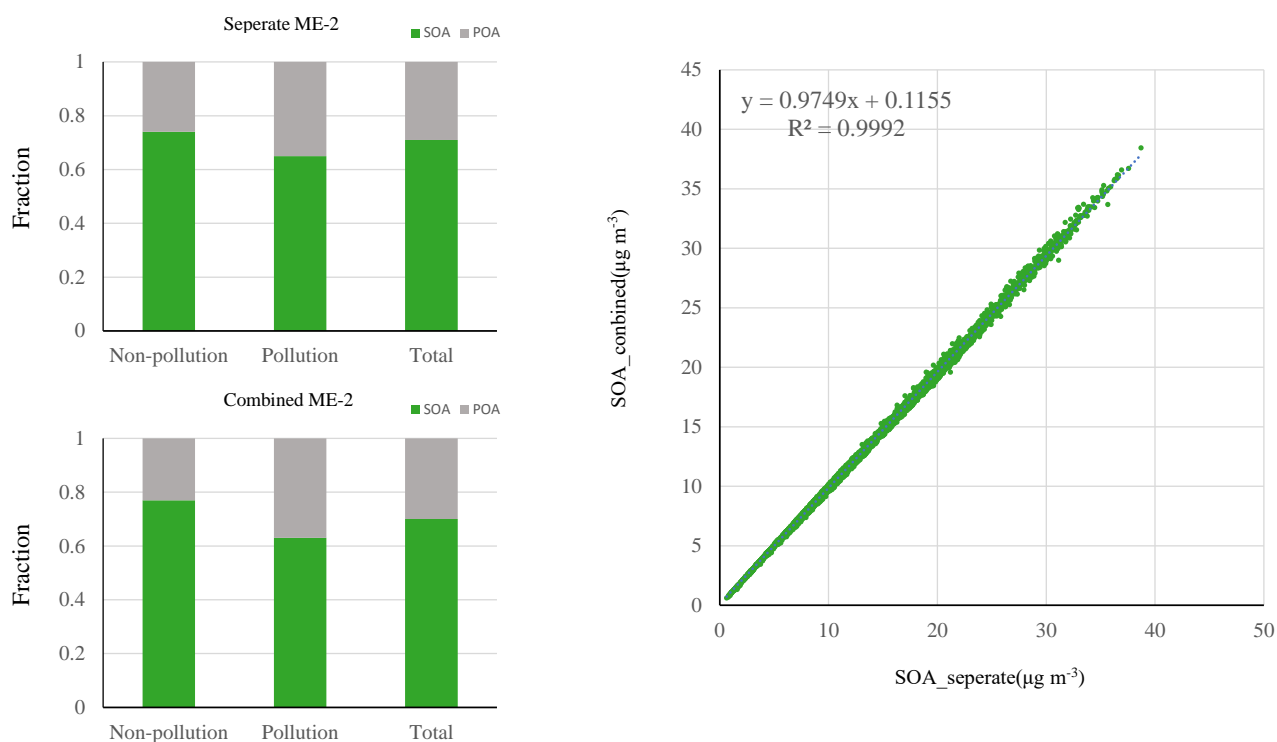
Figure S17. Comparison between combined ME-2 and separate ME-2, along with their correlations.

References

Aiken, A. C., DeCarlo, P. F., Kroll, J. H., Worsnop, D. R., Huffman, J. A., Docherty, K. S., Ulbrich, I. M., Mohr, C., Kimmel, J. R., Sueper, D., Sun, Y., Zhang, Q., Trimborn, A., Northway, M., Ziemann, P. J., Canagaratna, M. R., Onasch, T. B., Alfarra, M. R., Prevot, A. S. H., Dommen, J., Duplissy, J., Metzger, A., Baltensperger, U., and Jimenez, J. L.: O/C and OM/OC ratios of primary, secondary, and ambient organic aerosols with high-resolution time-of-flight aerosol mass spectrometry, Environ. Sci. Technol., 42, 4478–4485, 2008.

Atkinson, R. and Arey, J.: Atmospheric degradation of volatile organic compounds, Chem. Rev., 103, 4605–4638, 2003.

Brito, J., Rizzo, L. V., Morgan, W. T., Coe, H., Johnson, B., Haywood, J., Longo, K., Freitas, S., Andreae, M. O., and Artaxo, P.: Ground-based aerosol characterization during the South American Biomass Burning Analysis (SAMBBA) field experiment, Atmos. Chem. Phys., 14, 12069-12083, 10.5194/acp-14-12069-2014, 2014.

Budisulistiorini, S. H., Riva, M., Williams, M., Miyakawa, T., Chen, J., Itoh, M., Surratt, J. D., and Kuwata, M.: Dominant contribution of oxygenated organic aerosol to haze particles from real-time observation in Singapore during an Indonesian wildfire event in 2015, Atmos. Chem. Phys., 18, 16481-16498, 10.5194/acp-18-16481-2018, 2018.

Herndon, S. C., Onasch, T. B., Wood, E. C., Kroll, J. H., Canagaratna, M. R., Jayne, J. T., Zavala, M. A., Knighton, W. B., Mazzoleni, C., Dubey, M. K., Ulbrich, I. M., Jimenez, J. L., Seila, R., de Gouw, J. A., de Foy, B., Fast, J., Molina, L. T., Kolb, C. E., and Worsnop, D. R.: Correlation of secondary organic aerosol with odd oxygen in Mexico City, Geophys. Res. Lett., 35, 10.1029/2008gl034058, 2008.

Fang, B., Zhao, W.X.*, Xu, X.Z., Zhou, J.C, Ma, X., Wang, S., Zhang, W.J.*, Dean S. Venables, Chen, W.D. Portable broadband cavity-enhanced spectrometer utilizing Kalman filtering: application to real-time, in situ monitoring of glyoxal and nitrogen dioxide, Optics Express, 2017, 25, 26910-26922.

Lamsal, R. Martin, A. Van Donkelaar, E. Celarier, E. Bucsela, K. Boersma, R. Dirksen, C. Luo, Y. Wang: Indirect validation of tropospheric nitrogen dioxide retrieved from the OMI satellite instrument: insight into the seasonal variation of nitrogen oxides at northern midlatitudes, J. Geophys. Res. Atmos., 115 (2010), p. D05302

Valin, A. Russell, R. Cohen: Variations of OH radical in an urban plume inferred from NO2 column measurements, Geophys. Res. Lett., 40 (2013), pp. 1856-1860.

Ng, N. L., Canagaratna, M. R., Zhang, Q., Jimenez, J. L., Tian, J., Ulbrich, I. M., Kroll, J. H., Docherty, K. S., Chhabra, P. S., Bahreini, R., Murphy, S. M., Seinfeld, J. H., Hildebrandt, L., Donahue, N. M.,

DeCarlo, P. F., Lanz, V. A., Prévôt, A. S. H., Dinar, E., Rudich, Y., and Worsnop, D. R.: Organic aerosol components observed in Northern Hemispheric datasets from Aerosol Mass Spectrometry, Atmos. Chem. Phys., 10, 4625-4641, 10.5194/acp-10-4625-2010, 2010.

Ng, N. L., Canagaratna, M. R., Jimenez, J. L., Chhabra, P. S., Seinfeld, J. H., and Worsnop, D. R.: Changes in organic aerosol composition with aging inferred from aerosol mass spectra, Atmos. Chem. Phys., 11, 6465-6474, 10.5194/acp-11-6465-2011, 2011.

Reece, S. M., Sinha, A., and Grieshop, A. P.: Primary and Photochemically Aged Aerosol Emissions from Biomass Cookstoves: Chemical and Physical Characterization, Environ. Sci. Technol., 51, 9379-9390, 10.1021/acs.est.7b01881, 2017.

Rohrer, F., Lu, K., Hofzumahaus, A., Bohn, B., Brauers, T., Chang, C.-C., Fuchs, H., Häseler, R., Holland, F., Hu, M., Kita, K., Kondo, Y., Li, X., Lou, S., Oebel, A., Shao, M., Zeng, L., Zhu, T., Zhang, Y., and Wahner, A.: Maximum efficiency in the hydroxyl-radical-based self-cleansing of the troposphere, Nature Geosci., 7, 559-563, 10.1038/ngeo2199, 2014.

Saha, P. K., Reece, S. M., and Grieshop, A. P.: Seasonally Varying Secondary Organic Aerosol Formation From In-Situ Oxidation of Near-Highway Air, Environ. Sci. Technol., 52, 7192-7202, 10.1021/acs.est.8b01134, 2018.

Schaub, D., Brunner, D., Boersma, K. F., Keller, J., Folini, D., Buchmann, B., Berresheim, H., and Staehelin, J.: SCIAMACHY tropospheric NO_2 over Switzerland: estimates of NO_x lifetimes and impact of the complex Alpine topography on the retrieval, Atmos. Chem. Phys., 7, 5971–5987, https://doi.org/10.5194/acp-7-5971-2007, 2007.

Stone, D., Evans, M. J., Walker, H., Ingham, T., Vaughan, S., Ouyang, B., Kennedy, O. J., McLeod, M. W., Jones, R. L., Hopkins, J., Punjabi, S., Lidster, R., Hamilton, J. F., Lee, J. D., Lewis, A. C., Carpenter, L. J., Forster, G., Oram, D. E., Reeves, C. E., Bauguitte, S., Morgan, W., Coe, H., Aruffo, E., Dari-Salisburgo, C., Giammaria, F., Di Carlo, P., and Heard, D. E.: Radical chemistry at night: comparisons between observed and modelled HOx, NO3 and N2O5 during the RONOCO project, Atmos. Chem. Phys., 14, 1299-1321, 10.5194/acp-14-1299-2014, 2014.

Volkamer, R., Sheehy, P., Molina, L. T., and Molina, M. J.: Oxidative capacity of the Mexico City atmosphere – Part 1: A radical source perspective, Atmos. Chem. Phys., 10, 6969-6991, 10.5194/acp-10-6969-2010, 2010.

Yang, C., Zhao, W., Fang, B., Xu, X., Zhang, Y., Gai, Y., Zhang, W., Venables, D. S., and Chen, W.: Removing Water Vapor Interference in Peroxy Radical Chemical Amplification with a Large Diameter Nafion Dryer, Anal. Chem., 90, 3307-3312, 10.1021/acs.analchem.7b04830, 2018.

Yang, C., Zhao, W., Fang, B., Yu, H., Xu, X., Zhang, Y., Gai, Y., Zhang, W., Chen, W., and Fittschen, C.: Improved Chemical Amplification Instrument by Using a Nafion Dryer as an Amplification Reactor for Quantifying Atmospheric Peroxy Radicals under Ambient Conditions, Anal. Chem., 91, 776-779, 10.1021/acs.analchem.8b04907, 2019.

Ziemann, P. J., and Atkinson, R.: Kinetics, products, and mechanisms of secondary organic aerosol formation, Chem. Soc. Rev., 41, 6582-6605, 10.1039/c2cs35122f, 2012.

Zou, Y.; Deng, X. J.; Zhu, D.; Gong, D. C.; Wang, H.; Li, F.; Tan, H. B.; Deng, T.; Mai, B. R.; Liu, X. T.; Wang, B. G., Characteristics of 1 year of observational data of VOCs, NOx and O3 at a suburban site in Guangzhou, China. Atmos. Chem. Phys. 2015, 15, (12), 6625-6636.